Sustainable Processes Connect
ISSN: 3079-1421
2026, Article ID. 2026.0026, Cite as: https://doi.org/10.69709/SusProc.172727

SCIFINITI PUBLISHING

Research Article

OPEN ACCESS

A Comparison of Hot Dry and Transitional Season Solar Drying with A Modified V-Corrugated Solar Air Heater

Usman Aminu[1,*] **Muhammad Sani Abdulkadir**[1] **Hussein Muhammed**[1] **Umar Faruk Lawan**[2]

[1] Department of Mechanical Engineering Technology, School of Engineering Technology, Nuhu Bamalli Polytechnic, Zaria P.O. Box 1061, Nigeria
[2] Department of Water Resources and Environmental Engineering, Aliko Dangote University of Science and Technology, Wudil P.O. Box 3244, Kano, Nigeria

Article History
Received: March 12, 2025 Accepted: May 07, 2026 Published: May 21, 2026

Abstract
The thermal performance of solar air heaters can be substantially enhanced by modifying the absorber plate geometry, which increases the heat-transfer surface area and promotes airflow turbulence. This study investigated the seasonal drying performance of a modified V-corrugated solar air heater operating under natural convection for drying tomatoes in Kano, Nigeria. Experiments were carried out during the transitional season (October–November 2019) and the hot-dry season (April–May 2021) using ASHRAE 93-2003 testing procedures. The system consists of a V-corrugated aluminum absorber panel, an enclosed drying chamber equipped with three trays, and a chimney designed to enhance buoyancy-driven airflow. The results showed a maximum drying efficiency of 54.66% during the transitional season, while shorter drying durations of 10–12 h were achieved during the hot-dry season, compared with 16–22 h during the transitional season. For all experimental trials, the moisture content decreased from 95.65% to approximately 10%. While drying periods were much shorter during the hot-dry season, ranging from 10–12 h compared with 16–22 h during the transitional season, the maximum drying efficiency of 54.66% was obtained during the transitional season. During the hot-dry season, moisture removal was increased and drying time was shortened by 45–55% due to higher sun irradiation (1250–1350 W/m^2), higher ambient temperatures (38–39 °C), and lower relative humidity (<35%). By increasing airflow turbulence within the collector and expanding the effective heat-transfer area, the redesigned V-corrugated absorber plate enhanced thermal performance. Compared with traditional open-sun drying, visual evaluation of the dried products revealed better color retention, consistent texture, and superior resistance to dust and insect contamination. Additionally, compared to traditional open-sun drying, the suggested solar drier may shorten drying times by roughly 70–85%, according to literature comparisons. The results show that, for year-round tomato preservation in semi-arid areas and off-grid rural settlements, the designed passive solar drying system is an efficient, affordable, and environmentally friendly solution.

Keywords:
V-corrugated absorber plate; solar drying; solar air heaters; open sun drying; solar powered solution

1. Introduction

Sun drying is a viable and cost-effective method for preserving agricultural products, particularly in tropical regions with high solar irradiance. Enclosed solar dryers demonstrate superior performance compared with conventional open-sun drying in terms of temperature control, protection from contamination, improved product quality, and reduced drying time [1,2]. These advantages have made solar drying an increasingly attractive option for reducing post-harvest losses in developing countries [3,4].

Among various improvement strategies, modifying the absorber plate design in solar air heaters has proven highly effective in enhancing thermal efficiency by

* **Corresponding Author:**
Usman Aminu, Department of Mechanical Engineering Technology, School of Engineering Technology, Nuhu Bamalli Polytechnic, Zaria P.O. Box 1061, Nigeria, uaminu14@nubapoly.edu.ng; Tel.: +2348164444860

increasing the heat transfer surface area and promoting airflow turbulence. Corrugated and roughened absorber surfaces, such as V grooves, ribs, and artificial roughness elements, reduce laminar airflow and increase convective heat transfer [5,6]. Numerical and experimental investigations have demonstrated that such surface alterations can increase thermal efficiency by 30–50% over flat plate designs [7,8].

Solar drying has been widely employed for the preservation of high-moisture agricultural products, such as tomatoes, which are highly perishable and prone to rapid degradation. Indirect solar dryers with thermal storage enhance drying stability and improve energy efficiency [9]; Hossain and Bala [10] demonstrated that using a solar tunnel dryer for hot chili drying enhanced drying efficiency and product quality compared to traditional open-sun drying methods. Similarly, Forson et al. [11] tested the performance of a mixed-mode natural-convection solar crop dryer in tropical climates, demonstrating the promise of passive solar drying systems for agricultural uses. Nevertheless, most available studies have primarily focused on forced convection systems or short-term performance evaluations.

The performance of solar dryers varies seasonally, particularly in tropical regions where natural convection plays a dominant role. Drying rate and moisture diffusion are directly affected by changes in ambient temperature, relative humidity, and solar radiation intensity between the dry and transitional seasons [12–14]. Nevertheless, experimental data comparing seasonal drying performance using improved absorber plate geometries remain limited.

Northern Nigeria provides a suitable natural setting for evaluating seasonal performance due to its clearly defined hot, dry, and transitional seasons. Optimization of system design and operation in rural contexts requires a comprehensive understanding of how climatic variability influences solar dryer efficiency.

Therefore, this study aimed to:

1. Evaluate the drying efficiency and drying time of a modified V-corrugated solar air heater in Kano, Nigeria, using natural convection during hot-dry and transitional seasons.
2. Evaluate the impact of seasonal environmental factors (solar radiation, temperature, humidity) on tomato drying kinetics.
3. Evaluate the effectiveness of a low-cost passive system for year-round tomato drying in semi-arid locations.

As shown in Figure 1, this study evaluates the performance of a modified V-corrugated solar air heater for tomato drying under hot, dry, and transitional seasonal conditions in northern Nigeria.

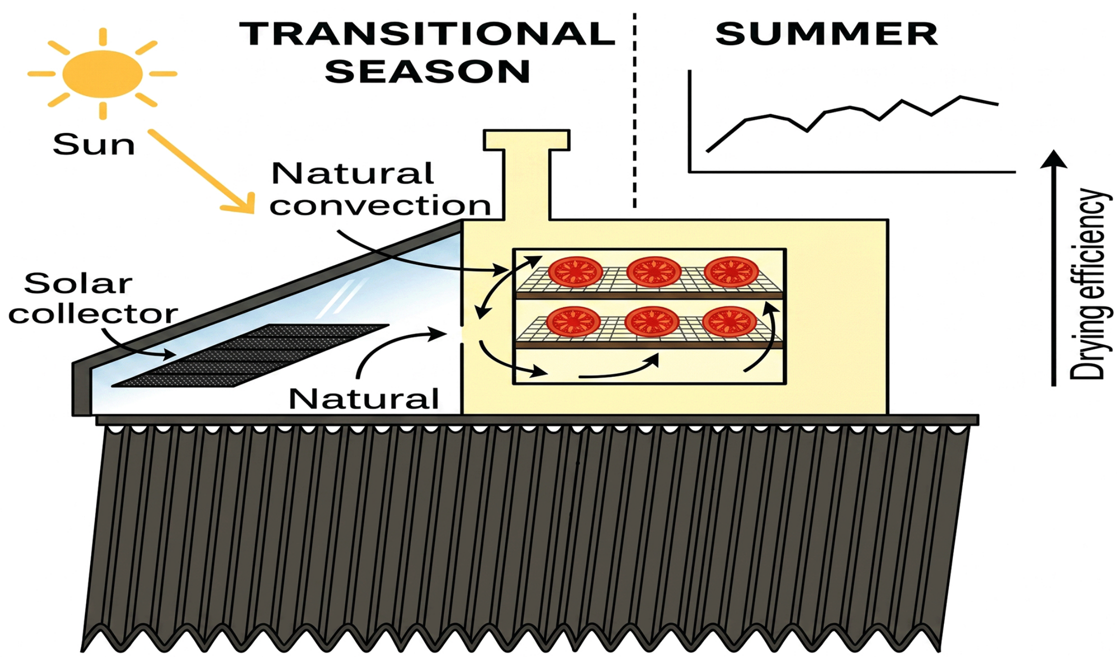

Figure 1: Schematic representation of solar drying performance during the hot dry and transitional seasons using a modified V-corrugated solar air heater.

2. Literature Review

Solar drying is a well-established, low-cost, and sustainable technique for post-harvest preservation of agricultural products, particularly in tropical and semi-arid areas. Indirect solar dryers offer advantages over open-sun drying by minimizing microbial contamination, improving product quality, and reducing drying time [1,3,4]. These benefits are achieved by separating the solar collector from the drying chamber, allowing better control of the drying environment.

2.1. Absorber Plate Modifications

A widely adopted approach for enhancing the thermal performance of solar air heaters is the use of corrugated or ribbed absorber plates, which increase the heat transfer surface area and promote airflow turbulence.

In a numerical study, Abedalh and Mohammed [5] reported that V-grooved corrugated absorber plates achieved 30–50% higher thermal efficiency than flat plates. Kumar et al. [7] experimentally investigated triangular corrugated absorbers under jet impingement and reported a thermal efficiency of 47.3%. In a related study, Assaye et al. [6] examined semi-circular transverse rib roughness on aluminium absorber plates and observed a thermal efficiency improvement exceeding 35%. Abdullah et al. [8] reported a 48% increase in thermal efficiency in a double-pass solar air heater through the use of delta wing turbulators.

Mahmood [15] reported significant improvements in outlet temperature and heat transfer coefficient in a double-pass unglazed solar air heater equipped with perforated plates and wire-mesh layers. Similarly, Karir et al. [16], in their review of arc-shaped rib roughness, concluded that turbulence-inducing modifications to absorber surfaces substantially enhance heat transfer performance.

2.2. Solar Dryers for Agricultural Products

Indirect solar dryers have been developed and experimentally evaluated for a variety of agricultural products. When compared to conventional open-sun drying techniques, Hossain and Bala [10] found that employing a solar tunnel drier to dry hot chilli improved drying performance and product quality. After reviewing several solar drying systems, El-Sebaii and Shalaby [9] found that adding thermal energy storage can increase drying continuity, lengthen drying times, and improve system performance. In Kano, Yahaya [17] developed and evaluated a multi-tray natural-convection dryer for yam drying and reported uniform product quality across trays, along with a significant reduction in drying time compared with open-sun drying.

In their assessment of solar dryers for marine and agricultural products, Fudholi et al. [4] concluded that indirect solar dryers consistently outperform open sun drying in terms of product quality, drying rate, and hygiene. For tomatoes and peppers, Forson et al. [11] developed a natural-convection indirect solar dryer that achieved more than 80% moisture removal within 48 hours. In a comprehensive review of solar energy drying systems, Ekechukwu and Norton [3] emphasized that appropriate collector design and effective airflow management are critical for achieving high drying efficiency.

2.3. Seasonal Performance Studies

Only a small number of research have looked into seasonal differences in solar dryer effectiveness. In their assessment of sun drying technologies, Janjai and Bala [18] underlined the necessity of taking environmental variability into account when designing and operating dryers, as well as the substantial impact of climatic circumstances on solar dryer performance. Bala and Woods [12] discovered that airflow velocity, solar radiation, and ambient temperature have a major impact on drier efficiency in their simulation of indirect solar drying. In a similar vein, greenhouse-style collectors can increase drying stability and heat retention, according to Jain and Tiwari [13].

2.4. Research Gap

The literature indicates that effective, hygienic, and rapid drying systems typically incorporate modified absorber plates, indirect drying chambers, well-managed natural or forced airflow, and transparent glazing materials.

Nevertheless, systematic research on tomato drying in northern Nigeria using a passive indirect solar dryer equipped with a V-corrugated absorber plate under varying seasonal conditions remains limited. By experimentally evaluating drying performance, moisture removal kinetics, and product quality during both hot-dry and transitional seasons, this study addresses the identified research gap. Table 1 summarizes selected solar dryer studies featuring modified absorber plates, highlighting the novelty of the present work.

Table 1: Summary of selected solar dryer studies with modified absorbers.

Author(s) (Year)	Absorber Type	Convection Mode	Product	Key Finding
Kumar et al. [7] (2023)	Triangular corrugated absorber	Forced	–	Achieved thermal efficiency of 47.3%
Abdullah et al. [8] (2018)	Turbulator-enhanced counter-flow double-pass solar air heater	Forced	–	Maximum daily thermal efficiency of approximately 68%
Abedalh & Mohammed [5] (2023)	V-grooved corrugated absorber	Forced/natural	–	Reported 30–50% improvement over flat-plate absorbers
Assaye et al. [6] (2022)	Semi-circular rib roughness	Forced	–	Achieved more than 35% enhancement in thermal performance
Hossain & Bala [10] (2007)	Solar tunnel dryer	Natural	Hot chilli	Improved drying performance and product quality compared with traditional open-sun drying
El-Sebaii and Shalaby [9] (2012)	Review of solar drying technologies	Various	Agricultural products	Reported that thermal energy storage may improve drying continuity and overall dryer performance
Kilanko et al. [17] (2019)	Flat-plate solar dryer	Natural	Yam	Demonstrated effective and relatively uniform multi-tray drying
This study	V-corrugated	Natural	Tomato	Comparative seasonal evaluation with maximum drying efficiency of 54.66%

3. Materials and Methods

3.1. System Description and Design

The experimental system was installed at Bayero University in Kano, Nigeria (11.9747° N, 8.4250° E). The device was a passive indirect solar dryer operating under natural convection, comprising a solar air collector, an insulated drying chamber, and an exhaust chimney.

3.1.1. Solar Air Collector

To maximize annual solar energy capture, the solar air collector was inclined at 15° to the horizontal, corresponding to the local latitude, and had dimensions of 1.5 m in length, 0.9 m in width, and 0.15 m in depth [13]. The collector frame was constructed from seasoned wood. A 4 mm thick transparent glass cover with a transmissivity of approximately 0.86 was installed to maintain high solar transmittance while minimizing convective and radiative heat losses. To minimize back and edge heat losses, the air duct beneath the absorber was lined with an aluminum sheet and insulated using 25 mm thick polyurethane foam with a thermal conductivity of approximately 0.023 W/m.K [1,3].

3.1.2. Modified V-Corrugated Absorber Plate

The primary component was a modified V-corrugated absorber plate with a solar absorptance of 0.95, fabricated from a 1.0-mm-thick aluminum sheet and coated with matte black paint (Figure 2). The corrugated geometry was designed to enhance convective heat transfer by increasing the effective heat transfer area and promoting airflow turbulence [5,6].

The geometrical parameters of the modified V-corrugated absorber plate were as follows:

- Corrugation pitch, P = 25 mm
- Corrugation depth, D = 20 mm
- Corrugation angle, β = 60°
- Effective absorber area (aperture area), Ac = 1.5 × 0.9 = 1.35 m^2
- Developed (actual) surface area ≈ 1.561.35 × sec(30°) ≈ 1.56 m^2 (∼16% increase over flat plate)

3.1.3. Drying Chamber and Chimney

The drying chamber, measuring 1.0 m in height, 0.6 m in width, and 0.5 m in depth, was constructed from 12-mm- thick plywood and insulated with 25-mm-thick polyurethane foam. The interior surfaces were lined with aluminum foil to enhance reflectivity and minimize heat loss. To ensure uniform airflow distribution, three perforated aluminum trays measuring 0.55 m × 0.45 m were installed with a vertical spacing of 15 cm between successive trays. To improve buoyancy-driven ventilation, a 1.2-m-tall PVC chimney with a diameter of 15 cm installed at the top of the drying chamber [11]. Figure 3 shows the solar dryer's schematic configuration, including the collector, drying chamber, trays, and chimney.

3.2. Instrumentation and Calibration

Prior to the commencement of the study, all instruments were calibrated in accordance with ASHRAE Standard 93-2003 [19]. Table 2 lists the instruments used for data collection, along with their specifications, accuracy, and calibration methods.

Throughout each drying experiment, data were manually recorded at hourly intervals between 09:00 and 18:00. The thermocouples were positioned at representative locations, including the collector inlet and outlet, the center of each tray, and the chimney exit. The anemometer was installed at the collector inlet and chamber outlet, while the pyranometer was mounted coplanar with the collector surface.

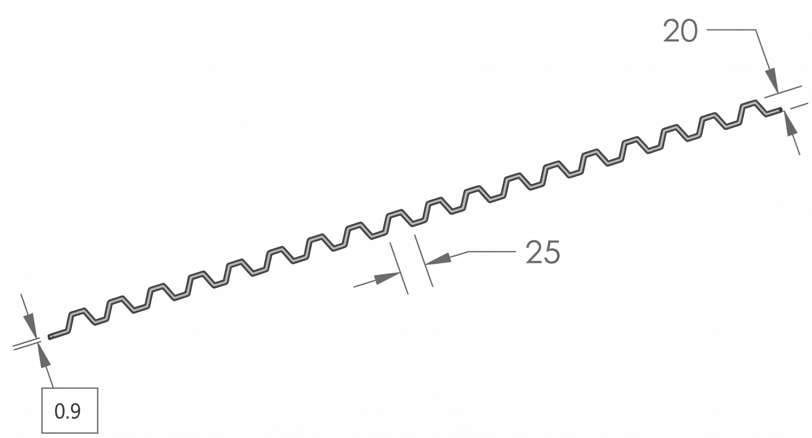

Figure 2: Modified V-shaped absorber plate.

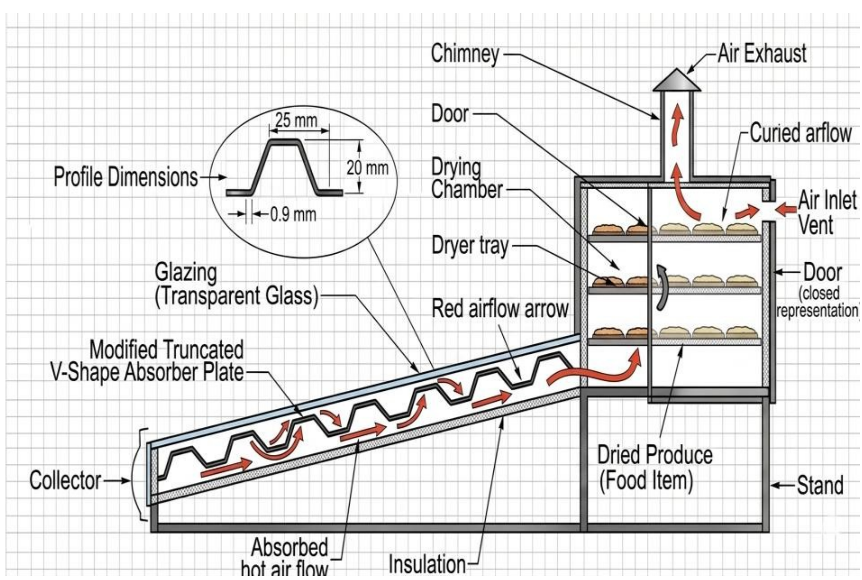

Figure 3: Schematic configuration of the solar dryer.

Table 2: Instruments used for measuring experimental parameters.

Parameter	Instrument	Model/Specification	Accuracy	Calibration Method
Solar radiation	Pyranometer	Kipp & Zonen CMP3	± 5 W/m^2	Factory calibrated, verified against reference cell
Temperature	Thermocouple	Type K (chromel-alumel)	± 1 °C	Ice-point (0 °C) and boiling-point (100 °C)
Air velocity	Digital anemometer	Testo 430	± 0.1 m/s	Controlled airflow bench
Relative humidity	Digital thermo-hygrometer	–	$\pm 3\%$ RH, ± 0.5 °C	Saturated salt solutions
Mass	Digital balance	–	± 0.01 g	Standard calibration weights

3.3. Experimental Procedure

3.3.1. Sample Preparation

Fresh Roma tomatoes (*Lycopersicon esculentum*) were procured from a local market in Kano. After selection based on uniformity in size, color, and ripeness, the tomatoes were washed with clean water and manually sliced to a uniform thickness of 5 mm using a stainless-steel knife. As illustrated in Figure 4, the initial moisture content was determined by oven-drying three 50 g samples at 105 ± 2 °C for 24 h [20]. The average initial moisture content was found to be 95.65% on a wet basis.

3.3.2. No-Load Tests

To characterize the maximum temperature rise and thermal performance of the collector under local environmental conditions, no-load tests (without product load) were conducted at the beginning of each experimental campaign. Hourly measurements were recorded for ambient temperature, wind speed, solar radiation, absorber temperature, and collector inlet and outlet temperatures.

3.3.3. Load Tests (Drying Experiments)

For each drying run, 1.5 kg of tomato slices was evenly distributed across the three drying trays. Drying experiments were performed in triplicate during two distinct seasonal periods:

- Transitional season: October–November 2019
- Hot dry season: April–May 2021

To assess the dryer performance under two different seasonal settings, the experimental campaigns were carried out in various years. Due to operational and logistical limitations related to research efforts during the COVID-19 pandemic, the hot dry season tests were not completed on time. To guarantee consistency and comparability of the results, however, the same dryer configuration, apparatus, calibration processes, and testing technique were kept throughout both experimental cycles.

Drying was continued until the sample mass reached a stable value, corresponding to a final moisture content of approximately 10% (wet basis), which is generally considered safe for storage [11]. Hourly measurements included:

- Solar irradiance, I (W/m^2)
- Ambient temperature, T_{amb} (°C) and relative humidity, RH (%)
- Collector inlet and outlet air temperatures, T_{in}, T_{out} (°C)
- Tray temperatures, tray1, tray2, Ttray3 (°C)
- Air velocity at collector inlet and chamber exit, v (m/s)
- Mass of each tray, m (g)

Figure 5 displays the experimental configuration used for the solar drying trials.

3.4. Data Reduction and Performance Evaluation

3.4.1. Moisture Content

Moisture content on a wet basis (wb) was calculated as:

$$MC_{wb} = \frac{m_W}{m_{wet}} \times 100\% \tag{1}$$

where m_w is the mass of water in the sample (kg), and m_t is the total mass of the wet sample at the corresponding measurement time (kg). Hourly moisture content was estimated from the recorded mass loss of tomato samples on each tray.

2026, Vol. 2, Article ID. 2026.0026
https://doi.org/10.69709/SusProc.172727

Figure 4: Tomato slices before drying.

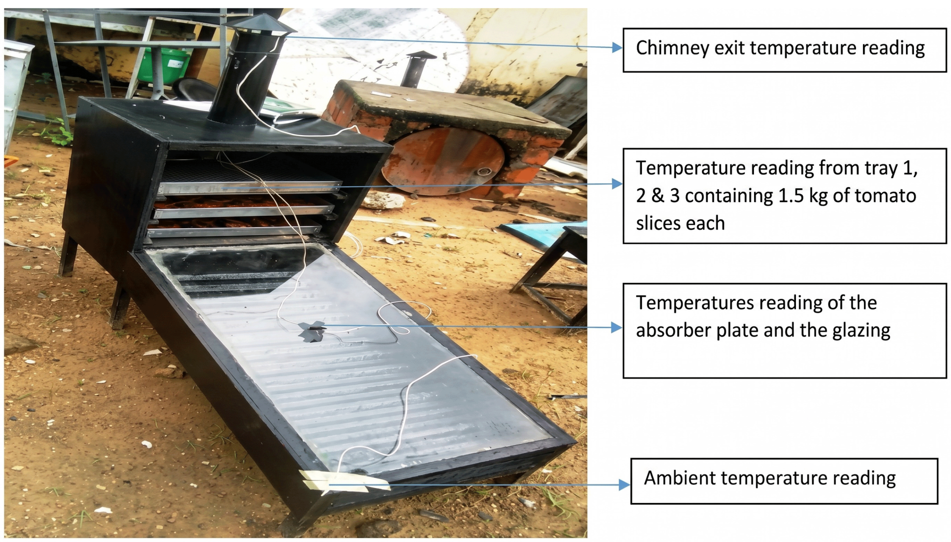

Figure 5: Experimental setup used for solar drying trials.

3.4.2. Drying Efficiency

The daily drying efficiency was calculated using the ASHRAE definition for solar collector systems adapted for drying [1]:

$$\eta_{dry} = \frac{M_w * L_v}{A_c \int Idt} \times 100\% \tag{2}$$

where:

- M_w = total mass of water evaporated during the drying period (kg)
- L_v = latent heat of vaporization of water at the average drying temperature (J/kg). For drying temperatures of 50–60 °C, $L_v = 2.37 \times 10^6$ J/kg [21]
- Ac = collector aperture area (1.35 m^2)
- $\int I\,dt$ = cumulative solar radiation incident on the collector plane during the drying period (J/m^2)

3.4.3. Air Mass Flow Rate

The air mass flow rate through the collector was calculated from velocity measurements at the collector inlet:

$$m. = \rho v A_{duct} \tag{3}$$

where ρ is air density (kg/m^3) calculated from ambient temperature and pressure, v is air velocity (m/s), and Aduct is the cross-sectional area of the collector inlet duct (0.9 m × 0.15 m = 0.135 m^2).

3.5. Statistical Analysis

All drying experiments were performed in triplicate. Results are reported as mean ± standard deviation (SD). SD was calculated as:

$$\mathrm{SD} = \sqrt{\frac{\sum_{i=1}^{n} (x_i - x^-)2}{n-1}} \tag{4}$$

where x_i is the individual measurement, x^- is the mean, and n is the number of observations (n = 3). One-way analysis of variance (ANOVA) was used to test for significant differences in drying efficiency between seasons at α = 0.05.

3.6. Uncertainty Analysis

Measurement uncertainties were propagated using the root-sum-square method [22]. The combined relative uncertainty in drying efficiency was estimated at ±5.2%, primarily arising from uncertainties in solar radiation measurements (±2.1%), mass measurements (±0.8%), and latent heat values (±1.5%).

4. Results

4.1. Environmental Conditions

Solar radiation was significantly higher ($p < 0.01$) during the hot dry season (average 1250–1350 W/m^2) compared to the transitional season (845–892 W/m^2). Ambient temperatures were 5–6 °C higher and relative humidity 20–25% lower during the hot dry season. Table 3 summarizes the average environmental conditions recorded during the drying experiments.

Table 3: Summary of average environmental conditions during drying experiments.

Experiment	Season	Month	Avg. Solar Radiation (W/m^2)	Avg. Ambient temp. (°C)	Avg. Relative Humidity (%)	Wind Speed (m/s)
1	Transitional	Oct 2019	845 ± 95	32.5 ± 1.8	58 ± 6	1.2 ± 0.3
2	Transitional	Nov 2019	892 ± 82	33.2 ± 1.5	52 ± 5	1.1 ± 0.2
3	Hot dry	Apr 2021	1245 ± 68	38.7 ± 1.2	35 ± 4	1.5 ± 0.3
4	Hot dry	May 2021	1318 ± 72	39.2 ± 1.1	32 ± 3	1.4 ± 0.2

4.2. No-Load Thermal Performance

Maximum absorber temperatures recorded during no-load testing were 82.7 °C in April and 83.7 °C in May, while lower values of 72.1 °C and 66.7 °C were observed in October and November, respectively. During peak solar radiation periods, the collector outlet air temperature exceeded ambient conditions by 25–30 °C, indicating effective heat transfer performance.

4.3. Drying Characteristics

4.3.1. Moisture Removal and Drying Time

Figure 6 illustrates the loss in weight of tomato slices following drying. The moisture content declined from an initial value of 95.65% (wet basis) to about 10% (wet basis) in all experimental trials, as assessed by weight loss. The corresponding drying times were:

i. October 2019: 22 h
ii. November 2019: 16 h
iii. April 2021: 12 h
iv. May 2021: 10 h

The hot dry season reduced drying time by 45–55% compared to the transitional season.

4.3.2. Drying Rate

The drying rate (kg water/h) was highest during the initial 2–3 h of each experiment, corresponding to the free moisture evaporation phase, and subsequently decreased progressively as bound moisture was removed. Maximum drying rates were 0.21 kg water/h in May, 0.19 kg water/h in April, 0.12 kg water/h in November, and 0.09 kg water/h in October.

4.4. Drying Efficiency

4.4.1. Daily Efficiency Variation

The daily drying efficiency for each experimental run is presented in Figures 7–10. Drying efficiency was highest during the initial stage of each trial when free surface moisture evaporated rapidly. Thereafter, efficiency decreased as the removal of bound moisture required greater energy input per unit mass of water removed.

4.4.2. Seasonal Comparison

On the first day of the October experiments, the highest drying efficiency of 54.66% was recorded. However, because drying was completed within fewer operating hours during the hot-dry season, the apparent day-1 drying efficiency was lower despite the faster moisture removal. In

2026, Vol. 2, Article ID. 2026.0026
https://doi.org/10.69709/SusProc.172727

fact, during the hot dry season, lower total energy was required per kilogram of water removed (Table 4).

Over the course of the experiments, drying time varied significantly. During the hot-dry season, drying was completed within 10–12 h due to higher solar irradiance, elevated ambient temperatures, and lower relative humidity. In contrast, during the transitional season, drying required approximately 16–22 h and typically extended over two to three days.

4.5. Product Quality Observations

4.5.1. Visual Assessment

i. Colour: Open sun-dried samples, exposed simultaneously on an adjacent tray, exhibited noticeable browning and darkening, whereas solar dried tomato slices retained their vivid red orange color (Figure 11).

ii. Hygiene: Solar-dried samples exhibited no evidence of dust, insect debris, or contamination. In contrast, samples exposed to open sun drying showed visible dust accumulation.

iii. Texture: Open sun-dried samples exhibited non-uniform drying, with some sections remaining moist, whereas solar dried slices showed uniform dryness and a leathery, flexible texture.

Although quantitative assessments of color and nutritional quality were outside the scope of this study, they are recommended for future research.

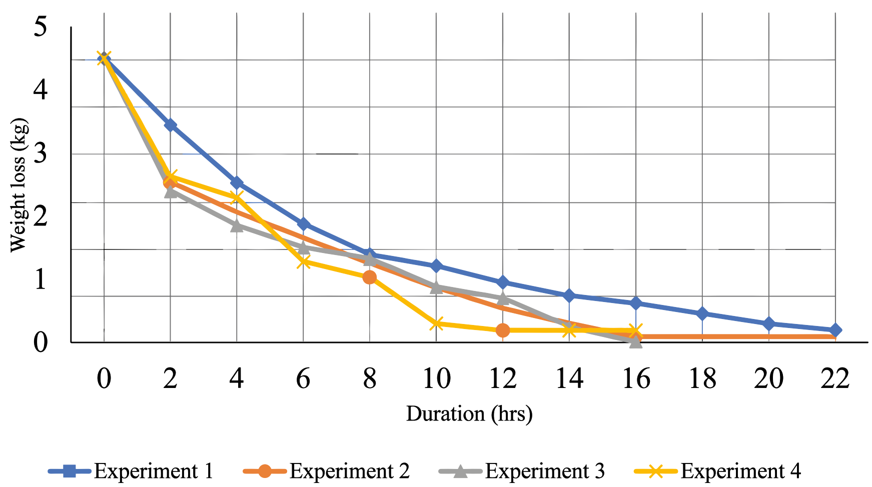

Figure 6: Weight loss of tomato slices in each of the four experimental scenarios during drying.

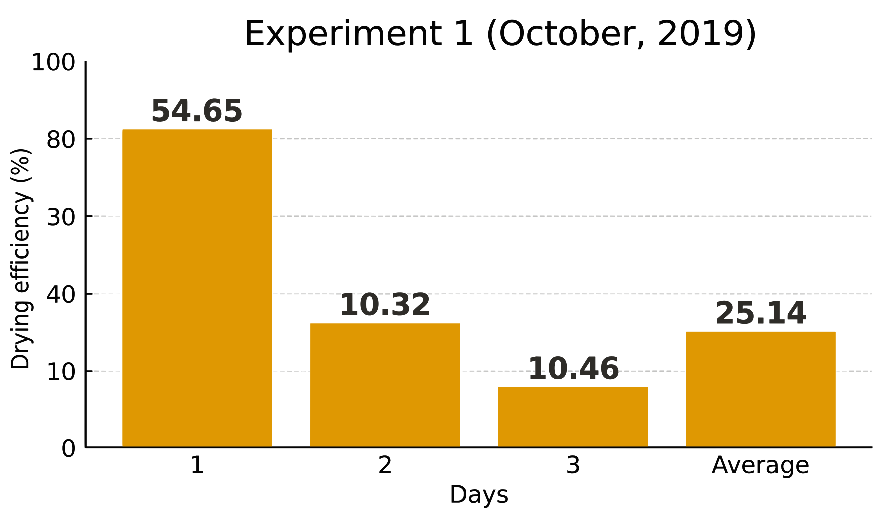

Figure 7: Daily variation of drying efficiency for experiment 1 (October 2019).

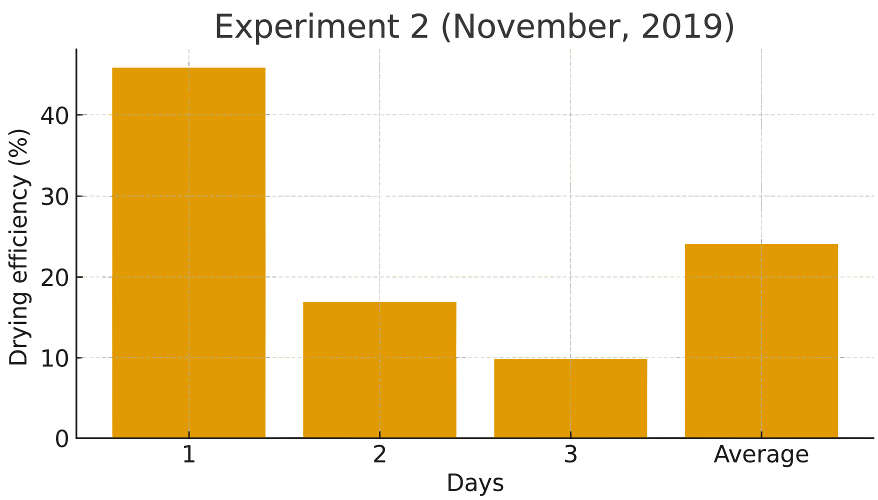

Figure 8: Daily variation of drying efficiency for experiment 2 (November 2019).

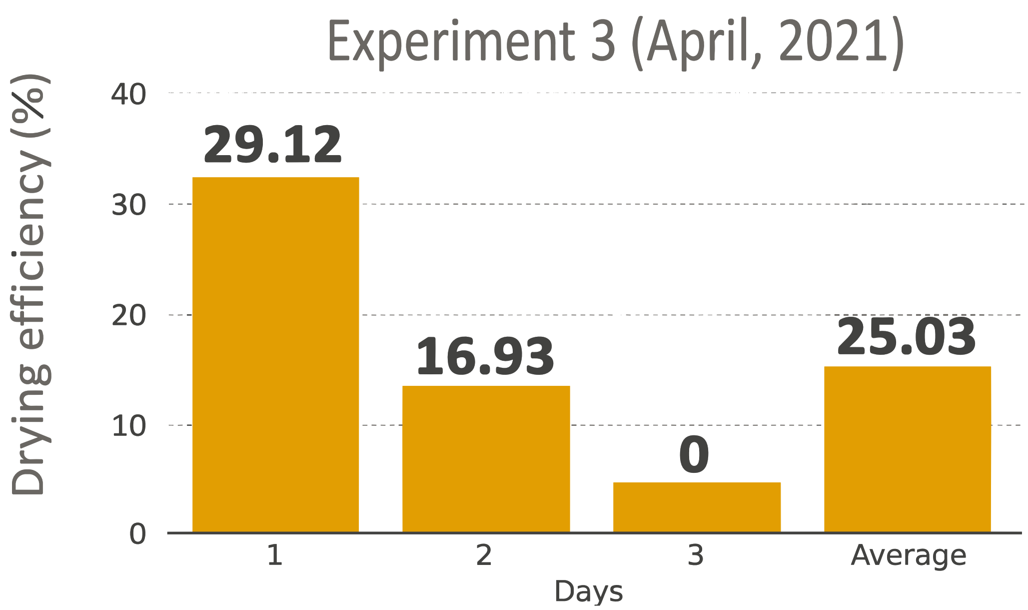

Figure 9: Daily variation of drying efficiency for experiment 3 (April 2021).

Table 4: Drying efficiency and drying time summary (mean $\pm$ SD, n = 3).

Experiment	Season	Month	Drying Time (h)	Day 1 Efficiency (%)	Day 2 Efficiency (%)	Day 3 Efficiency (%)
1	Transitional	Oct	22	54.66 ± 2.13	10.32 ± 0.85	10.46 ± 0.92
2	Transitional	Nov	16	45.60 ± 1.87	16.93 ± 1.02	9.84 ± 0.76
3	Hot dry	Apr	12	29.12 ± 1.54	15.88 ± 0.91	–
4	Hot dry	May	10	31.26 ± 1.61	–	–

2026, Vol. 2, Article ID. 2026.0026
https://doi.org/10.69709/SusProc.172727

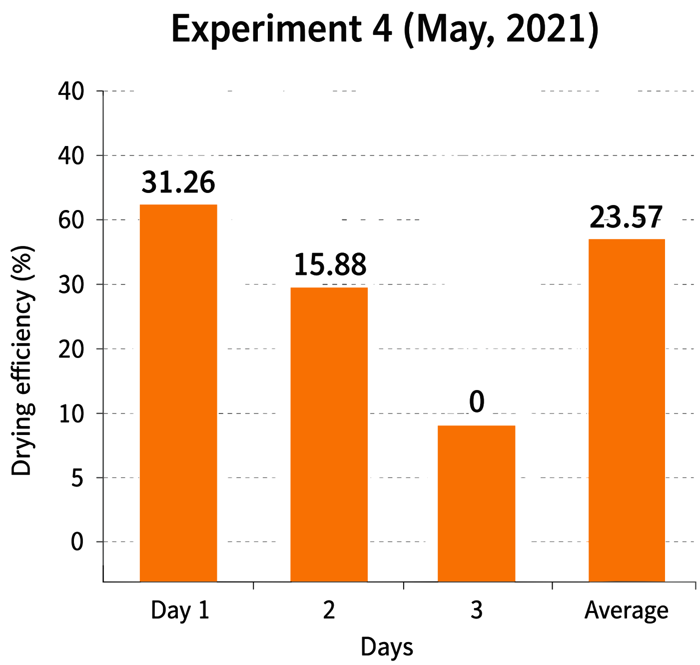

Figure 10: Daily variation of drying efficiency for experiment 4 (May 2021).

Figure 11: Tomato slices after drying.

5. Discussion

5.1. Effect of Seasonal Conditions on Drying Performance

The experimental findings demonstrate that the drying kinetics and efficiency of the passive V-corrugated solar dryer were significantly influenced by seasonal environmental factors, including solar radiation, ambient temperature, and relative humidity.

The average solar radiation during the hot dry season (April–May) exceeded 1250 W/m^2, with ambient temperatures approaching 40 °C and relative humidity below 35%. Moisture evaporation was accelerated under these conditions, leading to a strong vapor pressure gradient between the drying air and the tomato surface [12]. Consequently, drying time was reduced to 10–12 h, representing a 45–55% reduction compared with the transitional season.

The lower day-1 drying efficiency observed during the hot-dry season (29–31% compared with 45–55% in the transitional months) does not necessarily indicate inferior performance. Although a greater quantity of water was removed within a given time period, the corresponding instantaneous solar radiation input was also significantly higher. The hot dry season was more efficient in terms of energy consumption per kilogram of water removed (about 12–14 MJ/kg vs. 18–22 MJ/kg in the transitional season).

These results are in line with the observations made in the review by Janjai and Bala [18] and the modelling results of Bala and Woods [12], both of which emphasised the significant impact of sun radiation and ambient humidity on solar drying performance and drying kinetics

5.2. Role of the V-Corrugated Absorber Plate

The improved V-corrugated absorber plate enhanced the system's thermal performance through three mechanisms:

1. The corrugated profile provided approximately 16% greater absorber surface area than a flat plate with the same aperture area, increasing the effective heat-transfer area.
2. The V-groove geometry enhanced convective heat transfer by disrupting the laminar sublayer and generating localized turbulence between the absorber surface and the airflow [5,6].
3. The corrugated duct improved thermal mixing, minimized temperature stratification, and increased heat-transfer efficiency.

Comparable performance improvements have been reported for rib-roughened absorbers [6], triangular corrugated configurations [7], and V-grooved absorber designs [5]. The maximum drying effectiveness of 54.66% attained in this investigation is comparable to the 40.2% reported by Abdullah et al. [8] for delta wing turbulators and the 47.3% reported by Kumar et al. [7] for a forced convection triangular corrugated absorber. The improved performance of the present system may be attributed to the combined effect of natural convection, which avoids fan-related energy consumption, and the corrugation geometry, which enhances buoyancy-driven airflow and heat transfer.

5.3. Comparison with Open-Sun Drying

The suggested solar dryer may cut drying times by roughly 70–85% compared to traditional open-sun drying, according to literature comparisons; however, since systematic open-sun drying experiments were not carried out as part of the current study, this estimate should be interpreted cautiously. In the same vein, Hossain and Bala [10] reported that the drying performance and product quality were enhanced when a solar tunnel dryer was employed in comparison to conventional open-sun drying methods. Forson et al. [11] observed a 60–75% reduction in drying time for tomatoes using a natural-convection in-direct solar dryer. Additionally, contamination from dust, insects, and animals, which is a major quality limitation of conventional open-sun drying, was effectively prevented by the enclosed system design [3,4].

5.4. Practical Implications for Smallholder Farmers

For rural, off-grid communities in semi-arid areas, the system examined in this study offers the following benefits:

i. No electricity is needed: By eliminating the need for fans or blowers, passive operation minimizes both capital and operating costs.
ii. Local fabrication: The dryer can be constructed by local craftspeople using readily available materials such as wood, aluminum sheet, glass, and PVC tubing.
iii. Year-round usability: Farmers can preserve food even during periods of moderate solar radiation, as the system remains operational throughout the transitional season, although drying occurs more rapidly during the hot dry season.
iv. Scalability: To enhance drying capacity for larger crop loads, several collectors could be connected in parallel.

5.5. Limitations of This Study

Several limitations should be acknowledged:

i. No systematic measurements of moisture loss or drying time were conducted for open-sun-dried samples, although side-by-side visual comparisons were performed. As a result, the reported 70–85% reduction should be presented as a literature-based estimate rather than a direct experimental finding.
ii. Lycopene, vitamin C, and other heat-sensitive nutrients were not measured. Theoretically, their retention is expected to be improved due to shorter drying times and moderate temperature conditions; however, this has not yet been experimentally verified.
iii. The experiments were conducted exclusively in Kano, Nigeria; therefore, variations in microclimatic conditions or latitude may lead to different performance outcomes in other locations.
iv. The collector was operated for approximately 60 h in total; therefore, the long-term deterioration of the glazing and absorber coating was not assessed.
v. Drying efficiency was calculated based on total incident solar energy. However, some studies report moisture extraction rate or energy efficiency

instead; therefore, comparisons with such studies should be made with caution.

6. Conclusions

This study evaluated the seasonal drying performance of a modified V-corrugated solar air heater operating under natural convection for tomato drying in Kano, Nigeria. The following conclusions are drawn:

i. By enhancing airflow turbulence and increasing the effective heat transfer area, the redesigned V-corrugated absorber plate (60° corrugation angle, 25 mm pitch, and 20 mm depth) significantly improved thermal performance. A maximum drying efficiency of 54.66% was achieved.
ii. The passive sun drier decreased tomato moisture content from 95.65% to roughly 10% (wet basis) in every trial. Compared to the transitional season, drying periods during the hot dry season were 45–55% shorter. Furthermore, compared to traditional open-sun drying, literature comparisons indicate that the suggested solar dryer may shorten drying times by roughly 70–85%; however, direct experimental confirmation was outside the purview of this work.
iii. During the hot-dry season, higher ambient temperatures (38–39 °C), lower relative humidity (<35%), and higher sun radiation (>1250 W/m²) greatly improved moisture removal and shortened drying times to 10–12 h.
iv. In every experiment, the passive solar dryer reduced the moisture content of tomato slices from 95.65% to approximately 10% (wb). Compared with open-sun drying times reported in the literature, drying time was estimated to be 70–85% lower.
v. Compared with open-sun-dried samples, the solar-dried tomatoes exhibited better color retention, more uniform texture, and no visible contamination, highlighting the hygienic advantages of enclosed drying systems.
vi. The low-cost passive design offers smallholder farmers in off-grid areas a sustainable postharvest preservation option and appears technically feasible for year-round operation under semi-arid conditions.

7. Recommendations

In light of the study's limitations and findings, the following recommendations are proposed for further research and development:

i. Use combined experimental and computational fluid dynamics (CFD) approaches to investigate the effects of varying corrugation pitch, depth, and angle on heating and drying performance.
ii. To enable drying during periods of low solar radiation and extend daily operating hours, incorporate phase change materials or sensible heat storage systems, such as pebble bed storage.
iii. Evaluate dryer performance for other high-moisture crops, such as mangoes, onions, peppers, and okra.
iv. Compare natural and forced convection by retrofitting the system with a low-power photovoltaic (PV)-driven fan to evaluate the trade-off between energy input and drying rate.
v. To account for interannual climatic variability and establish reliable performance benchmarks, conduct evaluations over multiple years.
vi. Compare solar-dried and open-sun-dried tomatoes through laboratory analysis of key nutritional parameters, including vitamin C, lycopene, and β-carotene.
vii. Conduct a payback period analysis, scalability assessment, and full life-cycle cost evaluation to support adoption by smallholder cooperatives.
viii. To promote technology adoption, develop simplified construction guidelines and conduct practical training workshops for local artisans and farmers.

List of Abbreviations

ASHRAE	American Society of Heating, Refrigerating and Air-Conditioning Engineers
CFD	Computational Fluid Dynamics
L_v	Latent Heat of Vaporization
M_w	Mass of Water Evaporated
PV	Photovoltaic
PVC	Polyvinyl Chloride
RH	Relative Humidity
SD	Standard Deviation
wb	Wet Basis

Nomenclature

Symbol	Description	Unit
Ac	Collector Aperture Area	m^2
I	Solar Irradiance	W/m^2
$I*t$	Cumulative Solar Radiation	J/m^2
L_v	Latent heat of Vaporization of Water	J/kg

M_w	Mass of Water Evaporated	kg
t	Drying Time	h
ηdry	Drying Efficiency	%
θ	Collector Tilt Angle	°
P	Corrugation Pitch	mm
D	Corrugation Depth	mm
β	Corrugation Angle	°

Author Contributions

Conceptualization: U.A.; Methodology: U.A.; Data curation: U.A., H.M.; Investigation: U.A.; Formal analysis: M.S.A.; Validation: M.S.A.; Visualization: M.S.A.; Software: H.M.; Resources: H.M.; Supervision: U.F.L.; Project administration: U.F.L.; Writing—original draft preparation: U.A.; Writing—review and editing: M.S.A., H.M., U.F.L. All authors have read and agreed to the published version of the manuscript.

Availability of Data and Materials

Data associated with this article (hourly temperature records, solar radiation data, wind speed measurements, and complete weight loss data for all replicates) can be obtained from the corresponding author upon reasonable request.

Conflicts of Interest

The authors declare no conflicts of interest.

Funding

The study did not receive any external funding and was conducted using only institutional resources.

Acknowledgments

We praise Allah Ta'ala for the successful completion of this project. We are deeply thankful to Dr. Isa A. Yola, our supervisor, for his constant leadership, support, and invaluable critiques throughout this research. We are also grateful to Dr. A. I. Bashir and Prof. I. A. Rufa'i for their wisdom, tolerance, and insightful contributions. The authors sincerely thank Dr. Abubakar Shitu for his financial and in-kind support. We are incredibly appreciative of Alhaji Aminu Iro Paki, whose constant encouragement and impact have motivated us over our academic careers. May Aljannatul Firdausi be granted to him by Allah (SWT). We also appreciate Hajia Hassana Aminu, our dear mother, for her support, prayers, and encouragement. Finally, we appreciate everyone who contributed to this work, even if not specifically mentioned. May Allah accept and reward all sincere efforts.

AI Declaration

During the production of this work, the authors solely employed ChatGPT (OpenAI, version 2024) for language enhancement and grammatical correction. All scientific material, data interpretation, and creative contributions are the original works of the authors. The authors are solely responsible for the paper's final content.

References

[1] Fudholi, A.; Sopian, K.; Ruslan, M.H.; Alghoul, M.A.; Sulaiman, M.Y. Review of Solar Dryers for Agricultural and Marine Products. *Renew. Sustain. Energy Rev.* **2014**, *14*, 1–30. [CrossRef]

[2] Ekechukwu, O.V.; Norton, B. Review of Solar-Energy Drying Systems II: An Overview of Solar Drying Technology. *Energy Convers. Manag.* **1999**, *40*, 615–655. [CrossRef]

[3] Ekechukwu, O.V.; Norton, B. Review of Solar-Energy Drying Systems III: Low Temperature Air-Heating Solar Collectors for Crop Drying Applications. *Energy Convers. Manag.* **1999**, *40*, 657–667. [CrossRef]

[4] Fudholi, A.; Sopian, K.; Bakhtyar, B.; Gabbasa, M.; Othman, M.Y.; Ruslan, M.H. Review of Solar Drying Systems with Air Based Solar Collectors in Malaysia. *Renew. Sustain. Energy Rev.* **2015**, *51*, 1191–1204. [CrossRef]

[5] Abedalh, A.S.; Mohammed, S.H. Numerical Investigation of Thermal Performance of Solar Air Heater Using Different Angle V-Grooved Corrugated Absorber Plates. *Front. Heat. Mass. Transf.* **2023**, *21*, 227–243. [CrossRef]

[6] Assaye, M.; Biadgelegn, M.; Fekadu, B. Numerical Investigation of Convection Heat Transfer in a Solar Air Heater with Semi-Circular Transverse Rib Roughness. *Cogent Eng.* **2022**, *9*, 2106930. [CrossRef]

[7] Kumar, N.; Sharma, S.L.; Jasyal, N.K.; Debbarma, A. Performance Analysis of Solar Air Heater Using Triangular Corrugated Absorber under Jet Impingement. *Energy Sources Part A Recovery Util. Environ. Eff.* **2023**, *45*, 9063–9080. [CrossRef]

[8] Abdullah, A.S.; Abou Al-Sood, M.M.; Omara, Z.M.; Bek, M.A.; Kabeel, A.E. Performance Evaluation of a New Counter Flow Double Pass Solar Air Heater with Turbulators. *Sol. Energy* **2018**, *173*, 398–406. [CrossRef]

[9] El-Sebaii, A.A.; Shalaby, S.M. Solar drying of agricultural products: A review. *Renew. Sustain. Energy Rev.* **2012**, *16*, 37–43. [CrossRef]

[10] Hossain, M.A.; Bala, B.K. Drying of hot chilli using solar tunnel dryer. *Sol. Energy* **2007**, *81*, 85–92. [CrossRef]

[11] Forson, F.K.; Nazha, M.A.; Rajakaruna, H.; Navaratne, S.B. Modelling and Experimental Studies on a Mixed-Mode Natural Convection Solar Crop-Dryer. *Sol. Energy* **2007**, *81*, 346–357. [CrossRef]
[12] Bala, B.K.; Woods, J.L. Simulation of Indirect Solar Drying of Agricultural Products. *Sol. Energy* **1994**, *53*, 259–266. [CrossRef]
[13] Jain, D.; Tiwari, G.N. Effect of Greenhouse on Crop Drying under Natural Convection Conditions. *Energy Convers. Manag.* **2004**, *45*, 765–783. [CrossRef]
[14] Janjai, S.; Lamlert, N.; Intawee, P.; Mahayothee, B.; Bala, B.K.; Müller, J. Experimental and Simulated Performance of a PV-Ventilated Solar Greenhouse Dryer for Drying of Peeled Longan and Banana. *Sol. Energy* **2009**, *83*, 1550–1565. [CrossRef]
[15] Mahmood, A.J. Thermal Evaluation of a Double Pass Unglazed Solar Air Heater with Perforated Plate and Wire Mesh Layers. *Sustainability* **2020**, *12*, 3619. [CrossRef]
[16] Karir, R.; Rana, K.B.; Jain, P.K. A Comprehensive Review of Recent Trends in Augmentation Heat Transfer Solar Air Heaters Using Arc Shaped Ribs. In *Renewable Energy: Accelerating the Energy Transition*; Goyal, R., Patel, S., Sharma, A., Eds.; Springer: Singapore, 2023; pp. 45–62. [CrossRef]
[17] Kilanko, O.; Ilori, T.A.; Leramo, R.O.; Babalola, P.O.; Eluwa, S.E.; Onyenma, F.A.; Ameh, N.I.; Onwordi, P.N.; Aworinde, A.K.; Fajobi, M.A. Design and Performance Evaluation of a Solar Dryer. *J. Phys. Conf. Ser.* **2019**, *1378*, 032001. [CrossRef]
[18] Janjai, S.; Bala, B.K. Solar drying technology. *Food Eng. Rev.* **2012**, *4*, 16–54. [CrossRef]
[19] American Society of Heating, Refrigerating and Air-Conditioning Engineers. *ASHRAE Standard 93-2003: Methods of Testing to Determine the Thermal Performance of Solar Collectors*; American Society of Heating, Refrigerating and Air-Conditioning Engineers: Atlanta, GA, USA, 2003. Available online: https://webstore.ansi.org/preview-pages/ASHRAE/preview_ANSI+ASHRAE+93-2003.pdf (accessed on 15 June 2019).
[20] AOAC International. *Official Methods of Analysis of AOAC International*, 18th ed.; AOAC International: Gaithersburg, MD, USA, 2005. Available online: https://www.researchgate.net/publication/292783651_AOAC_2005 (accessed on 11 April 2020).
[21] Cengel, Y.A.; Boles, M.A. *Thermodynamics: An Engineering Approach*, 9th ed.; McGraw-Hill: New York, NY, USA, 2019. Available online: https://www.mheducation.com/highered/product/thermodynamics-an-engineering-approach-cengel.html (accessed on 9 July 2021).
[22] Taylor, J.R. *An Introduction to Error Analysis: The Study of Uncertainties in Physical Measurements*, 2nd ed.; University Science Books: Sausalito, CA, USA, 1997. Available online: https://mitpress.mit.edu/9780935702750/introduction-to-error-analysis/ (accessed on 15 June 2020).